Purinergic Signalling (2012) 8:677–692
DOI 10.1007/s11302-012-9298-3

ORIGINAL ARTICLE

Constitutive activity of the A_{2A} adenosine receptor and compartmentalised cyclic AMP signalling fine-tune noradrenaline release

Edin Ibrisimovic · Helmut Drobny · Qiong Yang · Thomas Höfer · Stefan Boehm · Christian Nanoff · Klaus Schicker

Received: 5 March 2012 / Accepted: 9 March 2012 / Published online: 5 April 2012

Abstract Neuroblastoma SH-SY5Y (SH) cells endogenously express A_{2A} adenosine receptors and can be differentiated into a sympathetic neuronal phenotype, capable of depolarisation-dependent noradrenaline release. Using differentiated SH culture, we here explored the link between A_{2A}-receptor signalling and neurotransmitter release. In response to the receptor agonist CGS21680, the cells produced cyclic AMP (cAMP), and when depolarised, they released increased amounts of noradrenaline. An A_{2A}-receptor antagonist, XAC, as well as an inhibitor of cAMP-dependent protein kinase A (PKA), H89, depressed agonist-dependent release. In the presence of XAC or H89, noradrenaline release was found to be below basal values. This suggested that release facilitation also owes to constitutive receptor activity. We demonstrate that even in the absence of an agonist, the native A_{2A}-receptor stimulated cAMP production, leading to the activation of PKA and enhanced noradrenaline release. Ancillary, non-cAMP-dependent effects of the receptor (i.e. phosphorylation of CREB, of Rabphilin3A) were refractory to constitutive activation. PKA-dependent facilitation of noradrenaline release was recapitulated with membrane-permeable 8-Br-cAMP; in addition to facilitation, 8-Br-cAMP caused marked inhibition of release, an effect not observed upon receptor activation. Inhibition by receptor-independent cAMP was likely due to suppression of voltagedependent calcium current (VDCC) and increased activity of Src-family kinases. Receptor-mediated release facilitation was reproduced in the presence of tetrodotoxin (blocking action potentials); hence, the signalling occurred at the active zone comprising release sites. Our findings thus support (1) presynaptic localisation of the A_{2A}-receptor and (2) suggest that compartmentalised pathways transmit cAMP signalling in order to facilitate depolarisation-dependent neurotransmitter release.

Keywords A_{2A} adenosine receptor · Neurotransmitter release · Presynaptic · Constitutive activity · Cyclic AMP · Signalling compartments · SH-SY5Y

E. Ibrisimovic · H. Drobny · Q. Yang · T. Höfer · S. Boehm · C. Nanoff (✉) · K. Schicker
Centre for Physiology and Pharmacology,
Institute of Pharmacology, Medizinische Universität Wien,
Währinger Strasse 13A,
1090 Wien, Austria
e-mail: christian.nanoff@meduniwien.ac.at

Introduction

In the central nervous system, adenosine dampens neuronal excitation, counteracts disinhibition by dopamine in the basal ganglia and promotes sleep. These effects arise from adenosine modulating neurotransmission via A_1 and A_{2A}-receptors. The A_1 receptor inhibits neurotransmission by membrane hyperpolarisation [1], and because this effect is so dominant, it has been proposed that adenosine acting via A_{2A}-receptors must have a discrete origin, likely through degradation of the co-transmitter ATP [2].

A_{2A} adenosine receptors modulate synaptic transmission in the basal ganglia. A major postsynaptic effect occurs through interference with dopamine signalling via the D_2 receptor [3], the inhibition of which has been ascribed to a membrane-delimited interaction of receptor proteins [4]. Moreover, A_{2A}-receptors have an impact on neurotransmitter release in the central and the peripheral nervous system [5]. In preparations of rat striatum (caudate nucleus and globus pallidus), A_{2A}-receptor activation modulates the release of several neurotransmitters, namely glutamate, γ-aminobutyric acid, acetylcholine [6–8] and dopamine [9], thus the receptor is in control of—and perhaps present on—several types of neurons.

A_{2A}-receptor-mediated control of neuromodulation encompasses both facilitation and suppression of neurotransmitter release. Within the striatum for instance, modulation of γ-aminobutyric acid release apparently depends on the nuclear region with inhibition occurring in the caudate nucleus and facilitation in the globus pallidus [8, 10–15]. Inhibitory activity is surprising because the A_{2A}-receptor, a G_s/G_{olf}-coupled receptor stimulating the production of cAMP, has signalling properties that are conducive to enhanced neurotransmitter release. Cyclic AMP targets, protein kinase A (PKA), exchange protein activated by cAMP (Epac/cAMP-GEF) and hyperpolarisation and cyclic nucleotide-activated (HCN) ion channels all are present in nerve cells and endowed with roles in release modulation. In neurons, PKA transmits the cAMP stimulus by priming proteins of the fusion apparatus by phosphorylation [16]; Epac physically associates to vesicular docking proteins and complements PKA as cAMP sensor stimulating exocytosis [16, 17]. Based on the effects of specific channel blockers, HCN activity may also be involved in presynaptic stimulation of neurotransmission [18, 19]. Alternatively, A_{2A}-receptors can generate signals independently of cAMP to activate extracellular signal-regulated protein kinases 1/2 (ERK) [20] and protein kinase C (PKC) [20–22]; PKC activation is a well-documented intermediate in facilitated noradrenaline release [23].

Region- or cell-specific differences may be due to the differential expression of specific accessory proteins, e.g. those receptors with which A_{2A}-receptors can crosstalk [24], or of others that couple the receptor to effects intermingling with release, namely receptor-mediated stimulation of neurotransmitter uptake [25]. Cells may differ in their expression pattern of G proteins and their (proximal or downstream) effectors. In addition, they may assemble specific compartments that predispose operation of an individual effector mechanism. Compartment building blocks include scaffold molecules, such as A-kinase anchoring proteins (AKAPs); AKAP subtypes cluster protein kinases and phosphatases, phosphodiesterases and even integrate G protein-coupled receptors in protein complexes dedicated to signal guidance [26, 27]. The presence of such compartments has been invoked to account for diverting the cAMP signal between PKA and Epac [16]; by analogy, compartments may dictate how the receptor impinges on neuromodulation, be it enhancing or inhibitory.

Due its effects on neurotransmitter release, it has been assumed that the A_{2A}-receptor is targeted to presynaptic sites of a neuron. Nevertheless, given the heterogeneity of nerve tissue preparations (e.g. brain slices), it is difficult to demonstrate with certainty that effects on neurotransmitter exocytosis stem from receptors situated in the presynaptic active zone. Tested drugs may elicit effects via receptors on the very neuron whose activity is being recorded, or alternatively they may act via the release of mediators from neighbouring (neuronal, glial or other types of) cells. This uncertainty has also been observed in synaptosomal preparations. Even with the use of relatively homogenous primary cell cultures, drug effects at neuronal soma or dendrites may contribute to the modulation of transmitter release by influencing cellular excitability [23]. Therefore, a prerogative for discriminating between presynaptic and non-presynaptic effects is disruption of electrical communication by blocking sodium channels with tetrodotoxin (TTX).

In order to explore the control of neurotransmitter release exerted by the A_{2A}-receptor, we used cultures of a clonal cell line derived from human neuroblastoma. SH-SY5Y (SH) cells endogenously express A_{2A}-receptors and differentiate to a nerve cell-like phenotype. SH cells are capable of propagating action potentials, sensitive to inhibition by TTX [28, 29]. According to their ontogeny, SH cells possess features of sympathetic nerves in that they synthesise, take up, store and release noradrenaline. They are amenable to measuring the release of noradrenaline under continuous superfusion, an assay format that prevents noradrenaline effects via autoreceptors [23]. Exploiting the cellular homogeneity of differentiated SH-cell culture, an established nerve cell model, we studied signalling by native A_{2A}-receptors and addressed their action in modulating noradrenaline release. In addition, we tested the hypothesis that the A_{2A}-receptor is endowed with a constitutive activity which we had previously reported for the cloned human receptor [30]. The effects we observed are all indicative of an action of a presynaptic receptor. Cyclic AMP/PKA signalling guided along subcellular compartments linked the receptor to noradrenaline release with its constitutive activity facilitating release, even in the absence of receptor agonists.

Materials and methods

The anti-CREB (cAMP-responsive element binding protein) monoclonal antibody (clone 48H2) and the rabbit anti-Rabphilin3A and anti-phosphotyrosine antibodies were all purchased from Sigma-Aldrich. Rabbit anti-phospho-Rabphilin3A (Ser234) was from Invitrogen (Paisley, UK). Anti-phospho-CREB (Ser133) monoclonal antibody (clone 10e9) was from Upstate (Temecula, CA, USA). Horseradish peroxidase-conjugated anti-mouse and anti-rabbit immunoglobulin antibodies were from GE Healthcare. The immunoreactive bands on nitrocellulose blots (from Whatman, Dassel, Germany) were detected using the SuperSignal chemiluminescence substrate from Pierce (Thermo Fisher Scientific). The Micro-BCA protein assay reagent kit also was from Pierce. The plasmids encoding the YFP (yellow fluorescent protein)-tagged catalytic and the CFP (cyan fluorescent protein)-tagged regulatory subunit of PKA [31] were a kind gift of Dr M. Zaccolo (Padova, Italy).

Materials for SDS–PAGE and electrotransfer were obtained from Bio-Rad (San Francisco, USA). Fetal calf serum was from PAA Laboratories (Linz, Austria); TurboFect transfection reagent from Fermentas, and cell culture media were purchased from Invitrogen. Bovine serum albumin (Cohn fraction V, BSA), all-*trans* retinoic acid (RA), CGS21680 (2-(4-(2-carboxyethyl)phenethylamino)-5′-*N*-ethylcarboxamidoadenosine), XAC (8-(4-(2-aminoethyl)aminocarbonylmethyloxy)phenyl-1,3-dipropylxanthine), GF109203X (bisindolmaleimide I), 8-Br-cGMP (8-bromoguanosine 3′,5′-cyclic monophosphate) and adenine nucleotides including 8-Br-cAMP (8-bromoguanosine 3′,5′-cyclic monophosphate), 8-pCPT-2′-O-Me-cAMP (8-(4-chlorophenylthio)-2′-O-methyladenosine-3′-5′-cyclic monophosphate) were from Sigma-Aldrich; adenosine deaminase and the type IV-selective phosphodiesterase (PDE) inhibitor Ro20-1724 (4-(3-butoxy-4-methoxybenzyl)-2-imidazolidinone) were from Roche Applied Science (Vienna, Austria); RA was dissolved in dimethyl sulphoxide and the solution was stored in aliquots at −80 °C. PP1 (1-*tert*-butyl-3-(4-methylphenyl)-1 h-pyrazolo[3,4-d]pyrimidin-4-amine), PP3 (4-amino-7-phenylpyrazol [3,4-d]pyrimidine) and K252A were from Calbiochem (Merck Biosciences). All other chemicals and reagents were of the highest purity grade available.

Cell culture

The SH-SY5Y neuroblastoma cell line was obtained from the European Collection of Cell Cultures (Salisbury, UK). SH cells were cultivated in Ham's F12/DMEM (1:1). Growth medium was supplemented with 15 % fetal bovine serum and 4 mM L-glutamine. To initiate differentiation into a nerve cell-like phenotype, the standard protocol involved two consecutive culture conditions, as proposed by Encinas et al. [32]; in phase 1, cells were cultured in growth medium supplemented with 10 μmol/l RA; in phase 2, cells were kept in serum-free medium (with no RA included) for a subsequent 48 h. The term differentiation always refers to culture subjected to this treatment. As it was virtually impossible to obtain reliable cell counts with differentiated cells (due to cell fragmentation upon manipulation), we estimated cell mass by determining protein yield from a culture dish. Transfection of cells was performed using TurboFect and according to the manufacturer's recommendations. For at least 20 h after transfection, cells were cultivated in growth medium with or without RA, prior to serum withdrawal and supplementing fresh medium.

Measurement of [^{3}H]noradrenaline release

[^{3}H]Noradrenaline uptake and superfusion were performed as described [33]. Differentiating cells were transferred to culture disks while cultivated in growth medium plus RA. Cells on disks were co-cultivated with SH cells seeded on the bottom of the same dish; serum plus RA was withdrawn after 24 h. After 2 days, the cultures were labeled with 0.05 μM [^{3}H]noradrenaline. After labelling, the culture discs were transferred to small chambers and superfused with a buffer containing 120 mM NaCl, 6.0 mM KCl, 2.0 mM $CaCl_2$, 2.0 mM $MgCl_2$, 20 mM glucose, 10 mM HEPES, 0.5 mM fumaric acid, 5.0 mM sodium pyruvate and 0.57 mM ascorbic acid, adjusted to pH 7.4 with NaOH. Collection of four minute fractions (superfusion rate was 1 ml/min) started after 60 min of washout. Tritium overflow was evoked during two consecutive stimulation periods (S1 and S2) by the inclusion of 40 mM KCl (NaCl was reduced accordingly to maintain isotonicity) for 60 s in the superfusion buffer. Where indicated tetrodotoxin (TTX; 0.1 μM) was added to the superfusion buffer after 50 min of run-in superfusion (i.e. 10 min before starting sample collection). Test reagents were routinely added 20 min before the second stimulation period if not indicated otherwise. At the end of experiments, the radioactivity remaining in the cells was extracted by immersion of the discs in 2 % (v/v) perchloric acid.

FRET microscopy

FRET (Förster resonance energy transfer) microscopy was performed as described previously [34]. Experiments were performed after transfection of RA-primed cells with the CFP/YFP double-tagged fluorescent PKA construct, followed by 48–72 h in serum-less medium. FRET images were recorded with a Zeiss Axiovert 200 M inverted epifluorescence microscope equipped with a Cool-SNAP fx cooled CCD camera (Photometrics, Roper Scientific, Tucson, AZ, USA). Microscopy was performed at room temperature on cells in fresh modified Krebs–Henseleit buffer (25 mM HEPES–NaOH, pH 7.4, 120 mM NaCl, 5 mM KCl, 1.2 mM $CaCl_2$ and 1.2 mM $MgSO_4$ supplemented with 5 mM D-glucose); the integration time was 100 ms per image. To determine the donor and acceptor spectral bleed-through values in the FRET setting, we individually imaged donor and acceptor single-transfected cells. Fluorescence images were background-corrected and analysed with the Wright ImageJ software (Wright Cell Imaging Facility, Toronto, Canada) PixFRET plug-in [35]. The FRET fluorescence signal was normalised for acceptor and donor intensity (FRET efficiency, NFRET). For quantification, we used the averaged intensity of the NFRET signal over the cell body.

Electrophysiology

Ca^{2+} currents were measured as described earlier [36]. Briefly, differentiated SH cells were continuously superfused at room temperature (20–24 °C) with recording buffer containing (mM): NaCl 120, tetraethylammonium chloride 20, KCl 3, $CaCl_2$ 2.5, $MgCl_2$ 2, HEPES–NaOH 10, glucose

20, tetrodotoxin 0.5 μM, pH 7.4 using a DAD-12 drug application system (Adams & List, Westbury, NY, USA) allowing for complete solution exchange which takes less than 100 ms in the vicinity of the studied cell [33]. CGS21680, 8-Br-cAMP or respective vehicle were included as indicated. For perforated patch clamp measurements, recording pipettes were pulled from borosilicate glass (Science Products, Frankfurt/Main, Germany) using a Flaming–Brown puller (Sutter Instruments, Novato, CA, USA). Pipettes were first front filled using a pipette solution containing (mM): caesium methanesulphonate 130, tetraethylammonium chloride 20, $CaCl_2$ 0.24, EGTA 5, glucose 10, HEPES–CsOH 10, pH 7.2. Subsequently, the electrodes were back-filled using the same solution containing 200 μg/ml amphotericin B (in 0.8 % DMSO). Pipettes filled that way had tip resistances of 3–4 MΩ. The resulting liquid junction potential between electrode and bath solution was calculated to be +15 mV and was corrected a priori.

Ca^{2+} currents were recorded using an Axopatch 200B amplifier and were digitised using a Digidata 1320 A/D converter and pClamp 10.2 software (all Molecular Devices, Sunnyvale, CA, USA). Cells were clamped to −80 mV and depolarised to 0 mV once every 15 s for 30 ms. The resulting currents were low-pass filtered at 2 kHz and digitised at 50 kHz. The resulting traces were analysed with pClamp 10.2 software.

Western blotting and immunoprecipitation

Cell lysates were prepared from SH culture differentiated in 10-cm dishes. Cultures were incubated with test reagents for 20 min (or a shorter period if indicated) in fresh serum-free medium including adenosine deaminase (1 U/ml). The incubation was terminated by aspiration of the medium, washing the cells with ice-cold PBS and clamp-freezing. After thawing, cells were scraped off the plastic support in 400 μl lysis buffer (50 mM Tris–HCl, pH 7.5, 1 mM EDTA, 150 mM NaCl, containing 0.5 % Nonidet P-40 substitute) containing phosphatase and protease inhibitors (PhosSTOP Phosphatase Inhibitor Cocktail, Complete from Roche Applied Science). After 15 min on ice, the lysate was cleared by centrifugation at 35,000×*g* for 10 min. Protein concentrations were determined using the BCA kit, and equal amounts of protein were applied to SDS–gel electrophoresis (assessing phosphorylation of CREB and of protein tyrosine residues).

For the precipitation of Rabphilin3A, we added anti-Rabphilin3A antibody at 2 μg/ml. After overnight incubation at 4 °C, protein A sepharose was added (100 μl of a 10 % slurry) (Roche Applied Science) and incubation was continued for a further 3 h at 4 °C. Sepharose was settled by centrifugation at 3,000 rpm, washed twice and the pellets resuspended in sample buffer used for SDS–gel electrophoresis.

After gel electrophoresis, proteins were transferred to a nitrocellulose membrane. Blots were developed with the phospho-protein antibodies. Following visualisation of anti-phospho-CREB and anti-phospho-Rabphilin antibodies, membranes were stripped using an acidic glycine solution (0.1 M, pH 2.5) and re-probed using antibodies directed against CREB and Rabphilin3A holo-proteins. Densitometry was performed with Wright ImageJ software (Wright Cell Imaging Facility, Toronto, Canada).

Measurement of cAMP and miscellaneous procedures

For the measurement of [^{3}H]cAMP, cells labelled with [^{3}H] adenine were processed as described [37]. Alternatively, cAMP was measured using an ELISA kit (R&D Systems, Minneapolis, MN, USA) according to the instructions provided by the manufacturer. In each experiment, we determined a calibration curve with increasing cAMP concentrations (3 to 200 nM). The absorbance of the coloured product was measured at a wavelength of 450 nm. Formation of cAMP was routinely assayed in the presence of Ro20-1724 (100 μM) and of adenosine deaminase (1 U/ml), at room temperature for 20 min. Statistical comparisons of mean values were carried out, as indicated, using the algorithms implemented in the SigmaPlot software (Systat Software, San Jose, CA, USA).

Results

SH cells endogenously express functional A_{2A} adenosine receptors; however, receptor signalling is contingent on cell differentiation, for which we utilised a protocol encompassing treatment with RA and serum starvation. Cells subjected to the differentiation protocol were growth-arrested and adopted a nerve cell-like phenotype, with phase-bright bodies and cellular processes that resembled neurite extensions [32]. We assessed receptor signalling by measuring activation of PKA. Using a double-fluorescent PKA construct, we followed the time course of the activity-dependent dissociation of regulatory and catalytic subunits. Agonist-dependent activation of the A_{2A}-receptor led to a decrease in FRET efficiency, which corresponds to activation of PKA. Figure 1a demonstrates that receptor activation prompted a significant FRET decrease only in differentiated cells (open triangles) whereas in undifferentiated, proliferating cells, the subtype-selective agonist CGS21680 (CGS) barely reduced the signal below controls (filled circles). Figure 1b depicts the false-colour image of a differentiated cell to document the marked change in FRET efficiency. The differentiation-dependent increase in receptor agonist efficacy was confirmed by measuring cAMP formation. Figure 1c depicts the agonist effect in a concentration-dependent manner in undifferentiated (filled circles) and

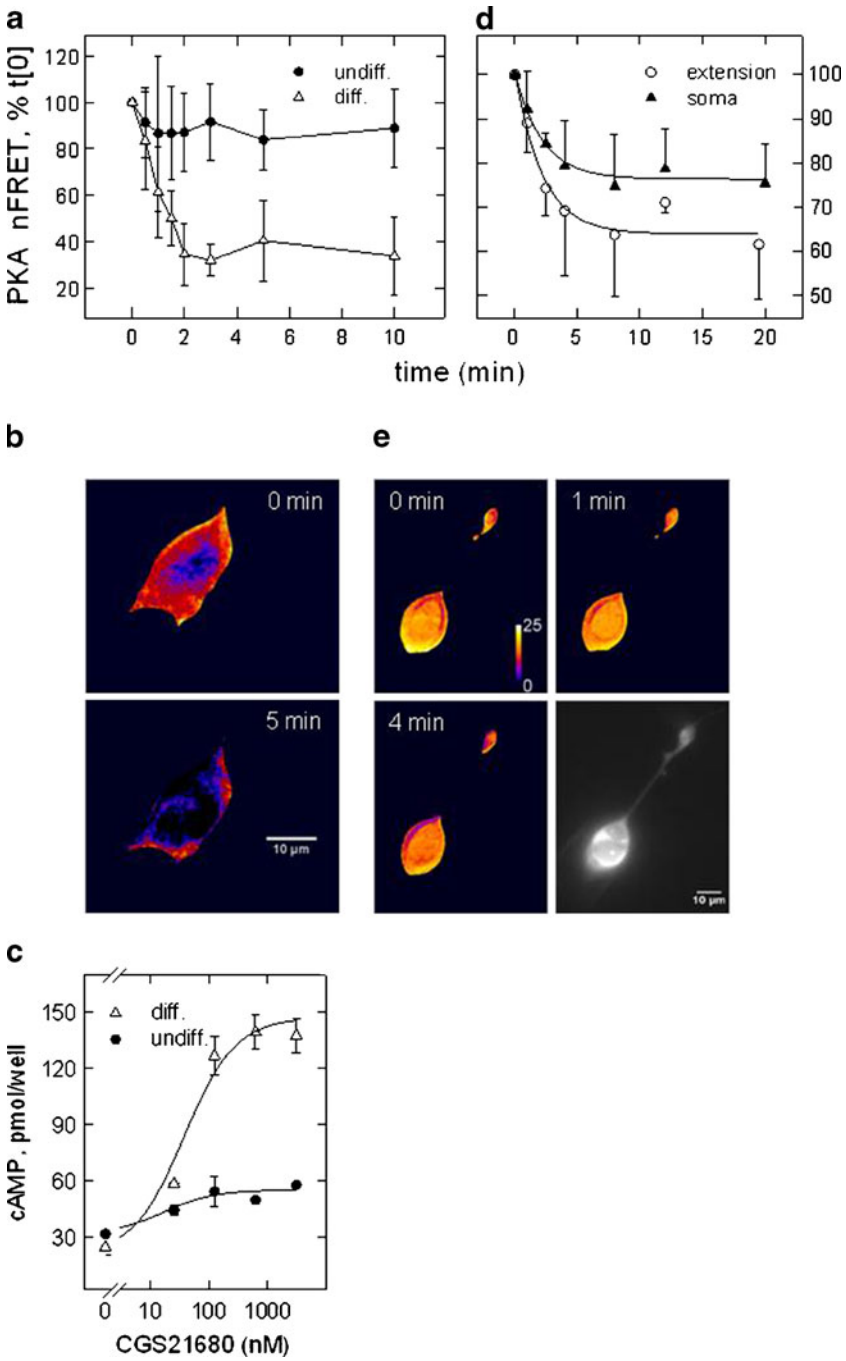

Fig. 1 A_{2A}-receptor-mediated activation of PKA and stimulation of cAMP formation in SH cells. FRET was recorded of the double-fluorescent PKA construct at various time points following addition of the A_{2A}-receptor agonist CGS21680 (0.5 μM). FRET values were normalised to the fluorescence intensity of donor and acceptor constructs. Plotted are mean values of FRET efficiency (NFRET means ± SD) expressed as percent of the value recorded before addition of the receptor agonist (set 100 %); the data points are connected by a spline curve for graphic purpose. In (**a**), the experiment was carried out in the presence Ro20-1724 (100 μM) to inhibit PDE activity. Shown are the means of six determinations obtained in differentiated (*open triangles*) and undifferentiated (*filled circles*) SH cells. In (**d**), experiments were performed without addition of Ro20-1724 (n=4). **b**, **e** Images of differentiated cells depicted in false-colour representation of FRET efficiency before and after the addition of the receptor agonist; red to blue transition signifies decreasing FRET efficiency. Images in (**b**) are representative of the time course depicted in (**a**) (times 0 and 5 min), images in (**e**) for the time course in (**d**) (times 0, 1 and 4 min). Image in *grey* tones (scale bar= 10 μm) depicts CFP (FRET donor) fluorescence to demonstrate that soma and a neurite extension are from the same cell. FRET-efficiency values for the PKA construct were in the range of 0.25–0.45. **c** Agonist-dependent formation of cAMP in the presence of Ro20-1724 in differentiated (*filled triangles*) and undifferentiated (*filled circles*) SH cells. Cyclic AMP was quantified in diluted cell lysates by ELISA

differentiated (open triangles) culture. Total amount and receptor-mediated increment of cAMP formation increased with differentiation corroborating the findings with the fluorescent PKA construct. The effective concentrations of CGS (EC_{50}=38 ± 15 nM) were consistent with activation of an A_{2A}-receptor subtype.

The experiments represented in Fig. 1a–c were carried out with a PDE inhibitor (Ro20-1724) and PKA activation resulted from accumulated cAMP. However, PKA activation was also detected in the absence of a PDE inhibitor. Figure 1d shows the summary of time course experiments performed in differentiated cells and in the absence of a PDE inhibitor where FRET was recorded from somata and neurite extensions, Fig. 1e gives representative false-colour FRET images at three time points. A_{2A}-receptor activation caused a parallel decline of the FRET signal in soma and neurites. The data show that decrement and effect rate were similar in both locations; both were more modest when compared to the experiment that included the PDE inhibitor (Fig. 1a–b, hue change to blue at 5 min). The bottom right panel of Fig. 1e gives a YFP image (from the FRET acceptor) to document that soma and extension were from the same cell. The data demonstrate that receptor agonist led to PKA activation in cell neurites and bodies and—because the time courses were similar—suggest that receptors were present in both locations.

Neuroblastoma originates from sympathetic precursors and SH cells express functional properties of a sympathetic neuron including depolarisation-triggered noradrenaline release [38]. Neurites and their boutons responded to receptor activation (Fig. 1e) and have been proposed to provide release sites [39, 40]. We therefore probed the effect of A_{2A}-receptor activation on noradrenaline release.

Figure 2a illustrates a release experiment carried out under continued superfusion. Two consecutive depolarisation stimuli (S1, S2) were delivered. When—starting 20 min before S2—the receptor agonist CGS21680 was included in the superfusion buffer, noradrenaline release increased. The insert in Fig. 2a demonstrates that the facilitating receptor action also occurred in the presence of tetrodotoxin (TTX, 100 nM) added to block voltage-dependent sodium channels.

The summary of S2/S1 ratios from a series of experiments is given in Fig. 2b (and in Table 2 where values are expressed as percent of controls). The receptor agonist-dependent increment was small amounting to ~14 % on an average (relative to vehicle, DMSO at 0.01 %). Although statistically significant, the increment was too small to confirm receptor specificity by varying the concentration of the agonist, CGS21680. However, the concentration we used (0.5 μM) was receptor subtype specific and maximally effective in stimulating cAMP formation (Fig. 1e). We confirmed that the effect was receptor specific by co-administering the antagonist XAC in release experiments. Addition of XAC

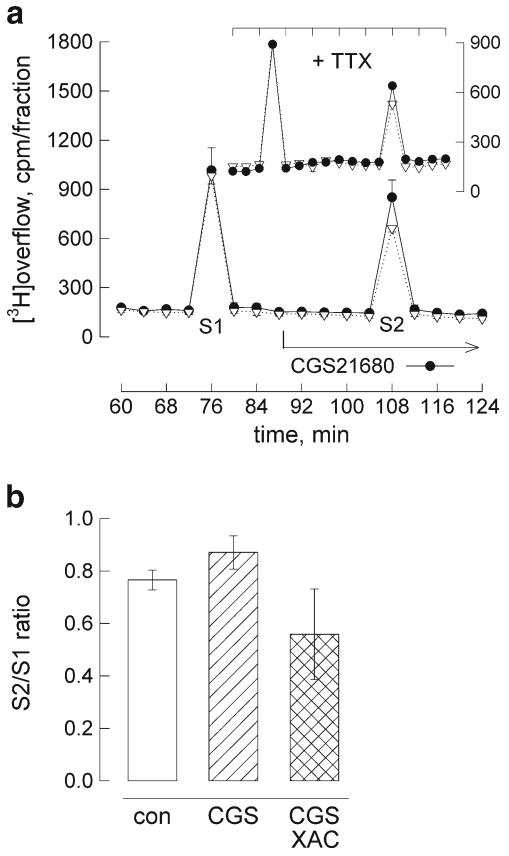

Fig. 2 Facilitation of depolarisation-triggered noradrenaline release. **a** Differentiated cells mounted on a plastic disk were superfused and superfused buffer was collected in four minute fractions. At 72 and 104 min, cells were depolarised by adding 40 mM KCl for 1 min. CGS21680 (0.5 μmol/l, *filled circles*) or vehicle (DMSO at 0.01 %, *open down-pointing triangles*) was included from minute 84 on (as indicated). The *insert* represents an experiment carried out on the presence of 100 nM TTX (+TTX) added together with the A_{2A}-receptor agonist. Plotted are the amounts of radioactivity per fraction; the results (means ± SEM) are from a single experiment performed in hexaplicates. **b** Summary of S2/S1 ratios obtained in release experiments with CGS21680 and XAC (5 μmol/l) added 20 min before S2. Results are from at least 12 determinations; *error bars* represent 99 % confidence intervals. An all-pairwise multiple comparison (Dunn's method) following one-way ANOVA revealed that mean values were significantly different from each other

(5 μM) suppressed the CGS21680 effect resulting in a S2/S1 ratio of 0.56 (the value was 0.87 in the presence of CGS21680; see Fig. 2b). Thus, XAC decreased noradrenaline release by 20 % to values that were below the appropriate controls (with an S2/S1 ratio of 0.77, Fig. 2b, Table 2); this suggests that XAC on its own modulated depolarisation-evoked noradrenaline release. Indeed, when we added XAC alone, release was lower than in controls (Fig. 3a, bar graph with control indicated by horizontal line, Table 2). The averaged S2/S1 ratios were similar when 5 μM XAC was included at S2 with (0.56, cross-hatched bar in Fig. 2b) or without CGS21680 (0.61; hatched bar in Fig. 3a).

We distinguished between the possibilities that XAC (1) displaced contaminating adenosine or (2) imparted inverse agonist activity on the A_{2A}-receptor. Contamination with adenosine at significant concentrations was less likely because cells were continuously superfused during the release experiment (flow rate=1 ml/min). Moreover, XAC also had an inhibitory effect when culture medium was pre-incubated with adenosine deaminase (1 U/ml) to degrade adenosine. Figure 3b shows formation of [^{3}H]cAMP in differentiated SH culture where no receptor agonist was added; after the addition of adenosine deaminase, cAMP formation was diminished by XAC (hatched bar) and, similarly, by the A_{2A}-receptor-selective antagonist ZM241385 (Fig. 3b, plot of concentration-dependent data). With either antagonist, the extent of inhibition amounted to one third the cAMP obtained with forskolin alone. The concentration range (IC_{50} ~0.7 ± 0.3 nM) was characteristic of ZM241385 binding to the human A_{2A}-receptor [30] and hence ruled out the involvement of an A_{2B} receptor. Thus, the basis for the inhibitory effects of XAC and ZM241385 in the absence of a receptor agonist was most likely in the constitutive activity of the A_{2A}-receptor which both antagonists can suppress [30].

As suggested above, monitoring PKA activity by FRET was a more sensitive means to detect A_{2A}-receptor activation than measuring cAMP. We tested the prediction further assessing constitutive receptor activity by PKA–FRET and did the experiment in the absence of a PDE inhibitor. Figure 3c shows PKA–FRET images of differentiated SH cells following the addition of ZM241385. We show three time series. Framed top rows are images (false-colour representation) of the uncorrected FRET signal showing a concentric distribution of the PKA sensor (reflecting central depth of the cell body). Two framed bottom rows show FRET-efficiency images (normalised for the PKA expression intensity) where the signal distribution appeared more even over the cell area. In both representations, changes in FRET were detected upon addition of the antagonist.

After a 20-min run-in period in fresh Krebs–Henseleit buffer plus adenosine deaminase (1 U/ml) during which the FRET signal was essentially stable (not shown), we added ZM241385 at 1 μM. PKA–FRET was recorded at 3-min intervals until after 15 min (Fig. 3d). FRET-intensity changes occurred in two types. Increased intensity in circumscribed areas (preferentially at cell margins, instances pointed out by arrows) and a wider diffraction halo around cell contours (due to signal amplification); both appeared in uncorrected and FRET-efficiency images. At 15 min, we added 8-Br-cAMP to revert the increase in FRET. 8-Br-cAMP reduced the FRET signal in cell regions that overlapped with and, in addition, were distinct from areas where the effect of ZM241385 had become apparent. This incongruence was possibly due to subcellular redistribution of PKA between recordings or due to differences in accessing PKA between 8-Br-cAMP and receptor-dependent cAMP.

From the samples shown, it is evident that addition of ZM241385 increased PKA–FRET. The extent of change was discrete and quick (not instantaneous) after addition of the antagonist. When we evaluated intensity changes over selected cell regions by densitometry, we find that values increased with time by 10 % to 20 % and were significantly different from time 0 at the last two time points (Fig. 3d). The findings substantiate the hypothesis that the human A_{2A}-receptor activates adenylyl cyclase in the absence of agonist and are suggestive of cAMP/PKA relaying receptor activity to release sites.

We therefore assessed the effect of inhibiting PKA and, in addition, used inhibitors of PKC and of the BDNF receptor, TrkB. Both PKC and TrkB have been reported to serve as ancillary effectors of A_{2A}-receptor signalling in nerve (cell-like) cells [21, 22, 24]. The A_{2A}-receptor can transactivate TrkB, which contributes to the functional adaptation of presynaptic nerve endings. We have verified that TrkB is functional in our cell line (by measuring a BDNF effect on ERK1/2; data not shown) as predicted [32]. On co-incubation with K252a, an inhibitor of TrkB kinase activity, A_{2A}-receptor activation significantly enhanced the release reaction (Table 1). Addition of K252a also increased basal release in the presence of XAC relative to controls (0.61, Fig. 3a). This effect may not be a consequence of TrkB inhibition as K252a also inhibits other kinases with high affinity (e.g. calmodulin-dependent kinase II). In the presence of K252a, the difference between CGS21680 and XAC was nevertheless significant providing evidence against an involvement of TrkB in facilitation [41]. Similarly, the PKC inhibitor (bisindolmaleimide I) failed to suppress release facilitation (Table 1). In contrast, when we co-administered the PKA inhibitor H89 (at a PKA-selective concentration, 1 μM), the S2/S1 ratio was ~0.6 in the presence of CGS21680 (Table 1). The values were similar to those obtained with XAC (cf. Fig. 3a). H89 applied together with XAC did not reduce noradrenaline release further (Table 1) which indicates that inhibition of PKA abolished receptor-dependent release facilitation suppressing its constitutive and agonist-dependent activity.

Thus, activation of PKA was sufficient to enhance noradrenaline release. In support of this, 8-Br-cAMP reproduced release facilitation by activating PKA. Figure 4a shows that H89 (open circles) reduced the amount of noradrenaline released when co-administered with 8-Br-cAMP (100 μM). The relative decrease (27 ± 5 %, mean ± SD, n= 3) and inhibition of receptor dependent release by H89 (~30 %) were comparable in size.

In addition to its facilitating action, however, 8-Br-cAMP also caused a second effect resulting in profound overall inhibition of noradrenaline release. Even in the absence of

H89, the net effect of 8-Br-cAMP was release inhibition relative to controls; concomitant PKA inhibition only magnified the extent of inhibition. Figure 4b shows that 8-Br-cAMP (100 μM) alone reduced the S2/S1 ratio on an average to ~0.5 (cf. Table 2); the effect of the direct activator of adenylyl cyclase, forskolin (10 μM), was similar (Fig. 4b). Inhibition of noradrenaline release by 8-Br-cAMP was reproduced in the presence of TTX (100 nM, not shown), which means that it was independent of action potentials.

Similar to the receptor action, the inhibitory mechanism due to receptor-independent cAMP was refractory to TTX inhibition and thus should take place close to release sites. We therefore measured calcium current that is prerequisite to vesicular exocytosis in the whole cell patch-clamp configuration and assessed the effects of 8-Br-cAMP and of CGS21680.

Figure 5 (right panel) and Table 2 show that 8-Br-cAMP inhibited voltage-dependent calcium current (VDCC). After addition of 8-Br-cAMP, inhibition gradually developed over 5 min curtailing ~20 % of the recorded calcium current (see Fig. 5, bar graph). VDCC inhibition of similar extent was sufficient to diminish voltage-dependent noradrenaline release from chick sympathetic neurons [42]. It is evident from Fig. 5 (left panel) that, contrary to 8-Br-cAMP, CGS21680 had no consistent effect on VDCC in SH cells even if present for an extended time interval (20 min). Thus, A_{2A}-receptor activation did not mediate release facilitation by increasing calcium influx; conversely, VDCC inhibition likely caused release inhibition by 8-Br-cAMP.

When stimulated with 10 μM forskolin, formation of cAMP amounted to levels 2-fold higher than those attained by receptor activation (manuscript submitted). However, inhibition by 8-Br-cAMP and forskolin were unlikely due to excess cAMP. Simultaneous inhibition of phosphodiesterase (to allow for cAMP accumulation) failed to reverse CGS21680-mediated facilitation. When Ro20-1724 was included, the receptor agonist did not inhibit but invariably and significantly enhanced noradrenaline release (data not shown). We therefore surmised that 8-Br-cAMP regulated an ancillary effector that was inaccessible to receptor-formed cAMP. As a premise, SH cells should afford compartments to guide receptor-dependent cAMP to a set of PKA moieties whose activation enhanced the release reaction. Cyclic AMP present outside the receptor-aligned signalling domain activated an ancillary effector responsible for suppressing release; this effector pathway was readily accessible only to receptor-independent—but not receptor-formed—cAMP.

Signalling compartments should also favour—relative to the effect of a diffusible cAMP analogue—receptor-mediated regulation of alternative effectors. We probed phosphorylation of the transcription factor CREB and of Rabphilin3A (Rabphilin), both cAMP-regulated molecules that control the expression of neural properties but are not involved in the modulation of neurotransmitter exocytosis [16]. Rabphilin is an 82-kDa protein associated to synaptic vesicles and is a substrate of PKA, of calmodulin-dependent and other protein kinases [43]. Figure 6a shows immunoblots of phospho-CREB and phospho-Rabphilin. CGS21680 increased phosphorylation of both CREB and Rabphilin. When compared to 8-Br-cAMP, CGS21680 had a more pronounced effect. The bar diagram in Fig. 6b illustrates the mean increments (±SD) estimated by densitometry (n=4 experiments). The difference held up after a 20-min (Fig. 5a) or a shorter incubation interval (7 min, not shown); this means that it was not due to different time courses of stimulation by CGS and 8-Br-cAMP. Thus, the receptor was more efficient than receptor-independent cAMP in driving phosphorylation of a presynaptic and of a predominantly nuclear protein. Therefore, the receptor and the structures required for signal partitioning must be located to somatic and presynaptic regions.

We assessed the nature of the extra-compartmental mechanism leading to inhibition of VDCC and noradrenaline release. Substitution of 8-Br-cAMP by the Epac-selective cAMP analogue, 8-pCPT-2′-O-Me-cAMP at 100 μM did not reproduce inhibition (nor did it produce a stimulating effect, not shown).

We also tested for the possibility that cAMP at high concentrations might result in activation of protein kinase G. When we administered 8-Br-cGMP (30 μM) at S2, there was little but insignificant inhibition of depolarisation-induced noradrenaline

Fig. 3 Constitutive activity of the A_{2A}-receptor. **a** KCl-induced [^{3}H] noradrenaline release was determined in the presence of XAC (5 μM, *filled circles*) or vehicle (DMSO at 0.01 %, *open down-pointing triangles*); experiment performed as in Fig. 2. Radioactive overflow is plotted per fraction (means ± SEM from six determinations), expressed as percent of radioactivity taken up by the cells. *Bar* to the *right* represents the averaged S2/S1 ratio when XAC was added at S2 (*error bars*=99 % confidence interval, n=15 determinations) with the *solid horizontal line* indicating the mean S2/S1 ratio in (vehicle) controls (*dotted area* represents lower confidence interval) taken from Fig. 2b. **b** Cellular formation of cAMP in the presence of forskolin (20 μmol/) and of increasing concentrations of the A_{2A}-receptor antagonist ZM241385. Shown are the means of three determinations (±SEM). *Bar* represents cAMP formation in the presence of forskolin and XAC (5 μM) (mean ± SEM, n=3) determined in the same experiment. **c** Recording constitutive receptor activity by means of PKA–FRET. Transfected differentiated SH cells were incubated in fresh Krebs–Henseleit buffer supplemented with adenosine deaminase (1 U/ml) and PKA–FRET was recorded at the indicated intervals after addition of ZM241385 (1 μM). No PDE inhibitor added. After 15 min, 8-Br-cAMP (100 μM) was added and fluorescence was recorded 15 min later. Three samples are shown in false-colour representation of normalised (*top*, FRET efficiency) and unnormalised FRET values (*middle* and *bottom panel*) together with a grey-tone CFP donor image. Normalised FRET values were in the range of 0.25–0.45. **d** Change in PKA–FRET following addition of ZM241385 (1 μM) determined by measuring averaged FRET intensity over six selected cell regions (as depicted in **c**). Given are mean changes (±SD) relative to time point 0, *asterisks* indicate significant change at 12 and 15 min (p<0.05 by all-pairwise multiple comparison according to Dunn's method following one-way ANOVA)

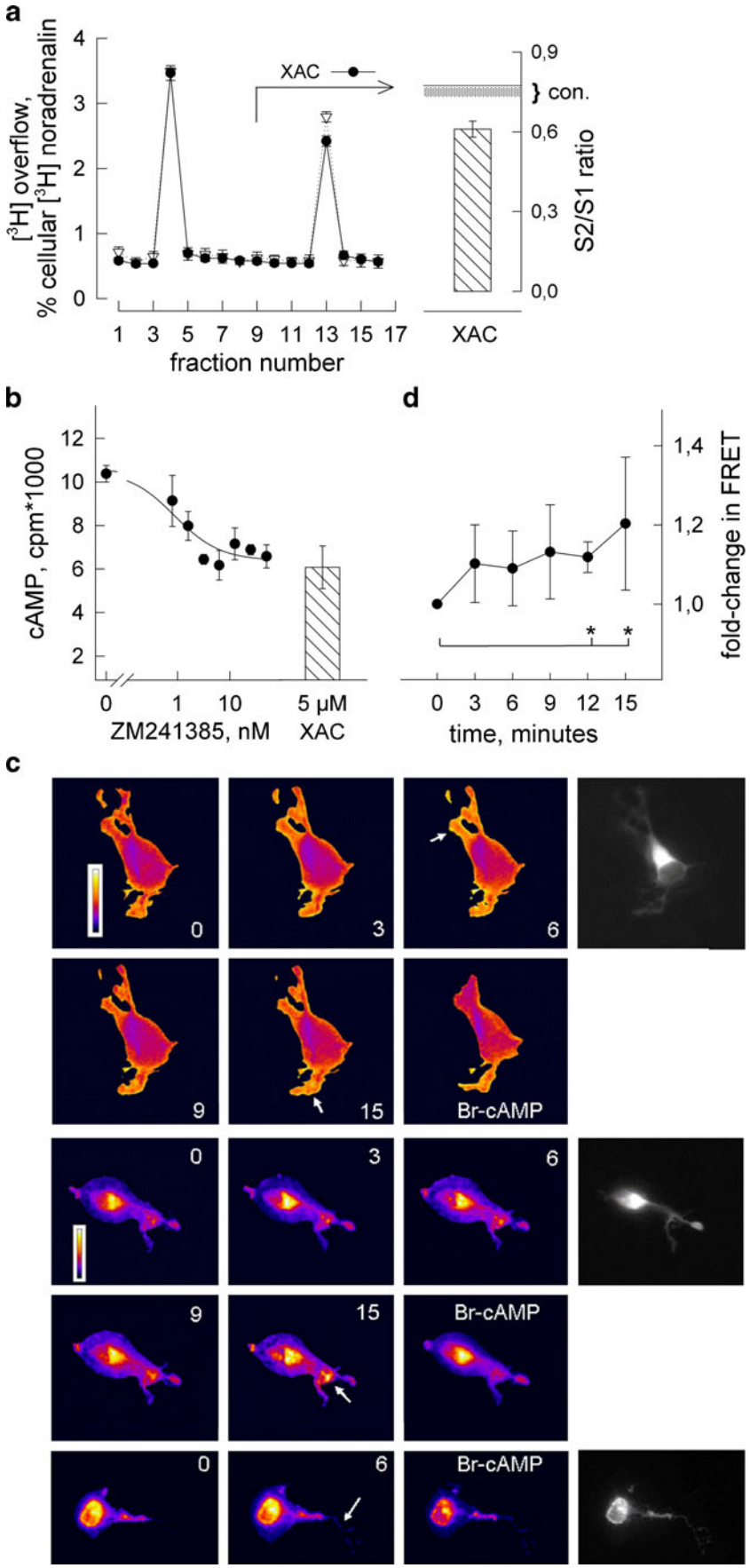
a
[3H] overflow, % cellular [3H] noradrenalin
XAC
} con.
S2/S1 ratio
fraction number
XAC
b
cAMP, cpm*1000
ZM241385, nM
5 μM XAC
d
fold-change in FRET
time, minutes
c
Br-cAMP
Br-cAMP
Br-cAMP

Table 1 Effect of protein kinase inhibitors on noradrenaline release

S2/S1	CGS21680	XAC
H89	0.58 (0.50–0.66)	0.56 (0.46–0.66)
Bisindolmaleimide I*	0.75 (0.66–0.84)	0.61 (0.58–0.64)
K252A*	0.97 (0.91–1.05)	0.85 (0.80–0.90)

Given are mean S2/S1 ratios (99 % confidence intervals from six to 15 determinations) in the presence of CGS21680 (0.5 μM) or XAC (5 μM) during S2. Inhibitors of PKA (H89, 1 μM), of PKC (bisindolmaleimide I, 1 μM) or of the TrkB receptor tyrosine kinase (K252A, 100 nM) were added concomitantly with CGS or XAC. Difference between CGS or XAC was significant (*$p<0.05$) in the presence of bisindolmaleimide I and K252A (Wilcoxon rank sum test)

release whereas a lower concentration of 8-Br-cAMP (3 μM) still produced inhibition (S2/S1=0.67 ± 0.05, mean ± SD). These findings argue against the involvement of PKG in cAMP-mediated inhibition.

Activity of Src-family kinases is a possible cause of release inhibition [44–46]. We tested the involvement of Src kinases by including the specific inhibitor PP1 in the release experiment and probing the effect of 8-Br-cAMP. Figure 4b shows that PP1 (1 μM) relieved inhibition due to 8-Br-cAMP. Noradrenaline release increased when co-administered at S2 and similarly when included in the superfusion buffer throughout the release experiment (not shown). We performed the following control experiments. (1) PP3, the PP1 analogue that does not inhibit Src-family kinases, was inactive in the release experiment; (2) PP1 alone did not affect basal release in the absence of 8-Br-cAMP (data not shown); (3) the effect of receptor activation was unaffected. S2/S1 ratios obtained with CGS21680 plus PP1 (0.75; CI=0.70–0.80) were somewhat lower than the values obtained in the absence of PP1 [0.8707 (0.8075–0.9339)]. However, this difference was not significant (multiple pairwise comparisons, ANOVA followed by Dunn's test). With XAC, the S2/S1 ratio in the presence of PP1 amounted to 0.63 (CI=0.55–0.71) and the difference between S2/S1 values in the presence of CGS and of XAC was significant (Table 1).

If 8-Br-cAMP exerted an inhibitory effect via Src-family kinases, it should also stimulate protein tyrosine phosphorylation in a manner sensitive to inhibition by PP1. We gauged the phosphotransfer reaction to protein tyrosine residues. Figure 7a shows immunoblots of cell lysates. In differentiated SH culture, 8-Br-cAMP increased the density of several phosphoprotein bands and co-incubation with PP1 reduced the intensity of most of them, e.g. of the predominant bands at ~60, 50 and 40 kDa. The receptor agonist CGS21680 also enhanced protein tyrosine phosphorylation. There were distinct differences, however, in the pattern of phosphoprotein bands and in the sensitivity of the phosphotransfer reaction to kinase inhibitors.

In two protein bands migrating in the range between 50 and 40 kDa (indicated by a star in Fig. 7a), phosphorylation increased marginally in the presence of CGS21680; in the presence of 8-Br-cAMP, the increase was robust. For other substrate proteins, the phosphorylation increment appeared concordant. From inspecting the blot in Fig. 7a, it becomes obvious that CGS-triggered phosphorylation was reduced by both PP1 and H89. None of the CGS-dependent (and

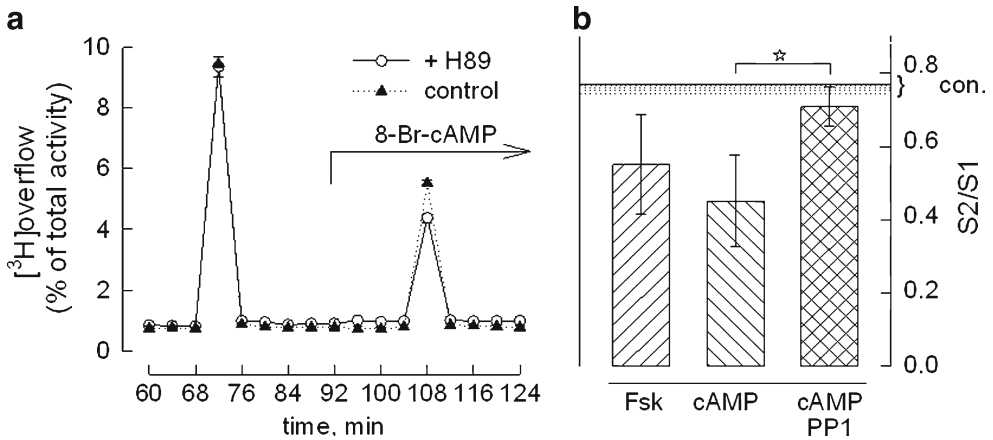

Fig. 4 Inhibition of neurotransmitter release by forskolin and 8-Br-cAMP. **a** Effect of PKA inhibition on noradrenaline release measured in the presence of 8-Br-cAMP. Shown is a superfusion experiment with 8-Br-cAMP (100 μM) alone (*filled triangles*) or 8-Br-cAMP together with H89 (1 μM, *open circles*; six determinations ± SEM). Collected radioactivity is expressed as percent of the total amount taken up by the cells. **b** Mean S2/S1 ratios of the depolarisation-induced noradrenaline release when forskolin (*Fsk*, 10 μM) or 8-Br-cAMP (*cAMP*, 100 μM) were added beginning 20 min before S2. The effect of 8-Br-cAMP was assessed in the presence of the Src-family kinase inhibitor PP1 (1 μM, *cross-hatched bar*). *Error bars* represent 99 % confidence intervals, $n \geq 12$. The *horizontal line* shows the mean S2/S1 ratio in controls; the *dotted area* represents the lower 99 % confidence interval taken from Fig. 2b. Release reduction by forskolin and 8-Br-cAMP was statistically significant relative to controls (Kruskal–Wallis one-way ANOVA followed by Dunn's test). *Asterisk* indicates that the effect of PP1 on release inhibition by 8-Br-cAMP was significant (relative to 8-Br-cAMP and forskolin)

Table 2 Effects, relative to basal, of CGS21680, 8-Br-cAMP and XAC on parameters measured in differentiated SH cells

Parameter	CGS21680	8-Br-cAMP	XAC
Cyclic AMP	5.6-fold (4.9–6.4-fold)	n.d.	61 % (41–81 %)
Noradrenaline release	114 % (105–122 %)	55 % (38–72 %)	80 % (69–91 %)
VDCC	101.9 ± 25.4 %	76.9 ± 16.4 %	n.d.
CREB phosphorylation	253 ± 65 %	140 ± 32 %	No effect[a]
Rabphilin phosphorylation	230 ± 58 %	132 ± 35 %	No effect[a]
Protein–tyrosine phosphorylation	168 ± 50 %	246 ± 84 %	No effect[a]

Effects presented in Figs. 1, 2, 3, 4, 5, 6 and 7 are expressed as percent of the appropriate basal value (except for cAMP in the presence of CGS21680)

[a] Repeated observations indicated that the amount of phospho-protein obtained in the presence of XAC was indistinguishable from basal (experiments performed in the presence of adenosine deaminase); 99 % confidence intervals are given in brackets, standard deviation as ±values. Statistical evaluation of differences is reported in the figure legends

prominent) phosphoprotein bands was refractory to inhibition by H89. Surprisingly, however, PKA inhibition was largely ineffective in the 8-Br-cAMP-induced phosphotransfer reaction.

We chose the predominant band at ~50 kDa to quantify inhibition by PP1 and H89. Figure 7b gives a summary of the densitometric analysis of three experiments comparing CGS and 8-Br-cAMP. The summary confirms that H89 discriminated between CGS and 8-Br-cAMP; H89 effectively blocked the effect of CGS only. By contrast, the Src inhibitor reduced the signal obtained with 8-Br-cAMP and inhibited CGS-dependent phosphorylation to a similar extent. The results suggest that 8-Br-cAMP activated Src-kinases with no requirement for PKA, which was similar to the mechanism operative in the inhibition of noradrenaline release. Src activation also occurred by the receptor, with PKA as possible signalling intermediate. PKA phosphorylation of Src is known to promote its release from the plasma membrane [47, 48] and PKA-directed Src activity has been implicated in downstream signalling of the A_{2A}-receptor [20]. The divergent mechanisms of Src activation support our hypothesis that receptor signalling is compartmentalised in differentiated SH cells; signal partitioning may thus provide the basis for facilitation of noradrenaline release by the A_{2A} adenosine receptor.

Discussion

The present study builds on a previous observation that cAMP formation is a regulated property in SH cells. Sensitised cAMP formation is the consequence of cell differentiation [49]. Only in differentiated cultures, the endogenous A_{2A} adenosine receptors robustly stimulated the formation of cAMP. Exploiting the nerve cell-like phenotype of

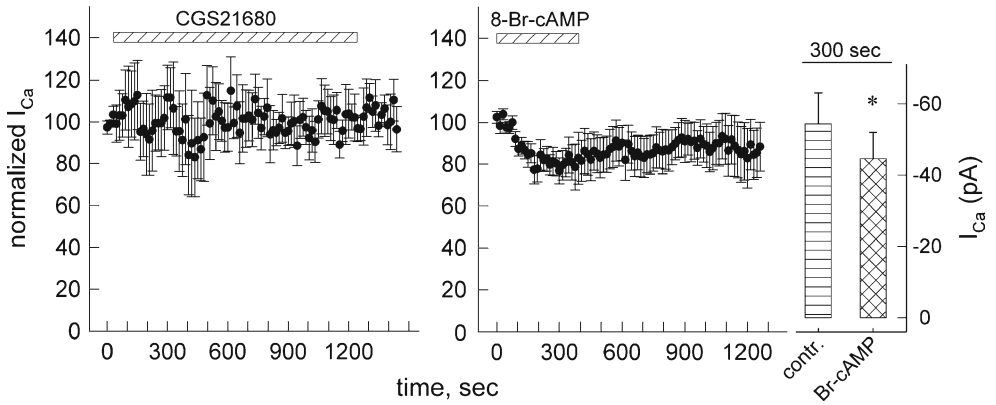

Fig. 5 Modulation of voltage-dependent calcium current. Shown are time courses with Ca^{2+} current measurements in differentiated SH cells. Single cells were voltage clamped to a holding potential of −80 mV using the perforated patch modification of the whole-cell patch clamp technique. Cells were continuously superfused with buffer containing DMSO (0.05 %) and were depolarised to 0 mV for 30 ms once every 15 s. After 60 s of baseline measurement, cells were either superfused with **a** CGS21680 (1 μM) for 20 min or **b** 8-Br-cAMP (100 μM) for 5 min. The recorded values were normalised to the mean of five baseline measurements. Given are mean values ± SEM from four recordings. Exposure to 8-Br-cAMP was terminated when the current levelled out to an apparent minimum. Bar graph (*right panel*) shows mean current values (±SEM) before and 300 s after addition of 8-Br-cAMP; *asterisk* indicates significant difference (n=7, p<0.05, Wilcoxon signed-rank test)

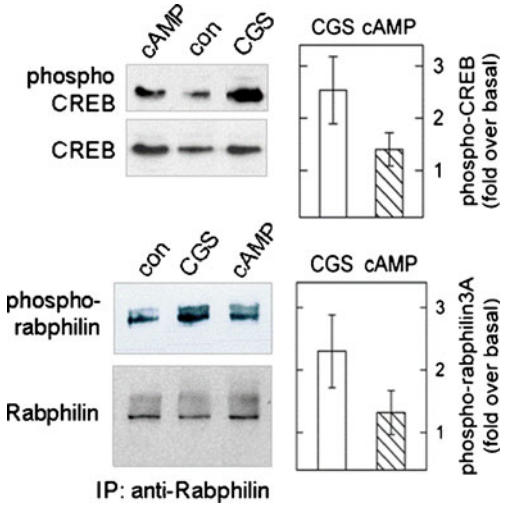

Fig. 6 Phosphorylation of CREB (serine 133) and of Rabphilin3A (serine 234) in differentiated SH cells. Phospho-CREB (migrating to a position of ~45 kDa) was determined by immunobloting cell extracts; Rabphilin3A was enriched by immunoprecipitation using an anti-Rabphilin3A antibody and detected with a specific anti-phospho-Rabphilin antibody. Differentiated cells were incubated with either CGS21680 (0.5 μM) or with 8-Br-cAMP (100 μM, cAMP) with no PDE inhibitor; after 20 min, the reaction was stopped by lysing cells. Shown are immunoblots from one sample out of four; phosphoprotein blots are shown above the corresponding blots developed with antibodies reactive to the holo-protein. The averaged results (±SD) of a densitometric analysis of band densities is given in the bar diagrams. Results are expressed (after correction for differences in sample loading) as relative increase over basal (cells incubated with 0.01 % DMSO in buffer). The differences between CGS (*open bar*) and 8-Br-cAMP (*hatched bar*) were statistically significant ($p<0.05$ by Student's *t* test) for both phosphoprotein bands. Irrelevant lanes were electronically removed from the figure representation; all lanes shown were from the same original immunoblot

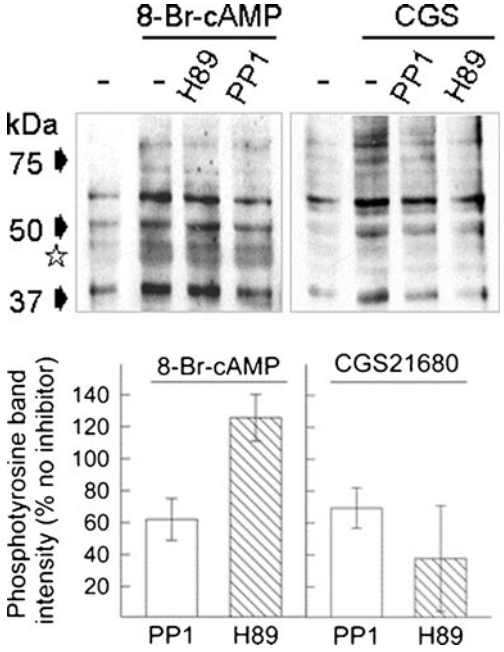

Fig. 7 Tyrosine phosphorylation in cell extracts from differentiated SH cells. *Top*—cells were incubated for 20 min with 8-Br-cAMP (100 μM, *left*) or with CGS21680 (0.5 μM, *right*) without PDE inhibitor. Immunoblots of cell lysates were developed with a phospho-tyrosine specific antibody. Controls (*leftmost lane*) were done with vehicle alone (−); H89 (1 μM) or PP1 (1 μM) were included in the incubation (following a 10-min pre-incubation) as indicated. The *asterisk* indicates a gel region with reagent-specific differences in phosphotyrosine bands. *Bottom*—bar diagram with the results of an analysis of the density changes in the band at ~50 kDa; shown is the average from three independent samples (±SD) where the effect of the kinase inhibitors (H89, *open bar*; PP1, *hatched bar*) on band density is expressed relative to the density obtained with 8-Br-cAMP (*left panel*) or CGS21680 (*right panel*) alone

differentiated SH cells, we assessed coupling of the A_{2A}-receptor to modulation of depolarisation-dependent neurotransmitter release and examined the role cAMP plays in this process. Our findings indicate that (1) the endogenous A_{2A}-receptor facilitates noradrenaline release in a manner compatible with a presynaptic type of action, that (2) signal compartments are present to guide receptor signalling and that (3) the native A_{2A}-receptor is endowed with constitutive activity.

The A_{2A}-receptor enhanced noradrenaline release and activation of PKA was necessary to relay the signal. Release facilitation via PKA was commensurate with A_{2A}-receptors located on neurite extensions (cf. Fig. 1b). Probably, release sites are present on SH-cell neurites, which were found to be rich in vesicles and proteins of the vesicle-fusion apparatus [39, 40]. Thus, A_{2A}-receptors may be located close to release sites and, in addition, they meet the criteria for docking to the 'presynaptic' active zone. First, receptor-dependent facilitation was refractory to the suppression of action potentials by TTX. Second, receptor activation led to the phosphorylation of presynaptic Rabphilin. Third, it has become clear that, in nerve cells, PKA targets proteins involved in vesicular fusion—rather than calcium channels as it does in endocrine cells—to enhance neurotransmitter release [16, 17]. In keeping with this consensus, the A_{2A}-receptor-dependent release facilitation was sensitive to the PKA inhibitor H89 and occurred without an effect on VDCC. Moreover, A_{2A}-receptor-triggered phosphorylation of Rabphilin, which is not considered an effector in regulated neurotransmitter exocytosis [16], was insensitive to H89 (data not shown). Taken together, these findings confirm a presynaptic type of action of the A_{2A}-receptor as stipulated previously, based on findings in preparations of rodent central (striatum, hippocampus, medulla and spinal cord) and peripheral nervous tissue (sympathetic nerve endings and motoneurons; [5, 50]) and attributed specifically to axon collaterals of striatal projections [51].

The A_{2A}-receptor revealed constitutive activity that enhanced noradrenaline release. In the absence of an agonist, receptor antagonists inhibited depolarisation-induced noradrenaline release, reduced cAMP formation and similarly diminished PKA activity. Hence, three types of experiment uniformly suggest constitutive activity and indicate that the

unoccupied A_{2A}-receptor was capable of generating cAMP. In keeping with the proposed sequence of events (receptor-dependent cAMP activates PKA to enhance noradrenaline release), inhibition of PKA and the receptor antagonist reduced noradrenaline to similar values and both were significantly lower than basal. Hence, permanent receptor activity sustained the quantum of neurotransmitter release.

We have previously detected constitutive activity on heterologous overexpression of the A_{2A}-receptor [30] and proposed that the active receptor conformation is favoured by the extended carboxy terminus; tight coupling to G_s probably supports the propensity for spontaneous signalling [52–54]. In mouse striatum, the A_{2A}-receptor couples to G_{olf} not expressed by SH cells ([55]; data not shown). Experiments in mouse striata lacking $G\alpha_{olf}$ suggest that G_{olf} itself has constitutive activity. It remains to be determined if constitutive receptor activity relies on the receptor coupling to a specific combinatorial assembly of heterotrimers (e.g. G_s or G_{olf}). Here, we confirm that constitutive activity is a trait of the native receptor protein that stimulates adenylyl cyclase via G_s. An argument repeatedly forwarded against constitutive adenosine receptor activity is contamination with adenosine, which would result in receptor agonist occupancy. Using radioligand displacement assays [37], we estimated that adenosine is present in culture supernatants at concentrations less than 10 nM, and that it is readily eliminated by adenosine deaminase (added at 1 U/ml, data not shown). In release experiments, we reduced contamination with adenosine by superfusing culture disks (suspended in chambers with an average volume of 150 μl) at a rate of 1 ml/min. With both methods mentioned, the antagonists (XAC and ZM241385) suppressed receptor activity.

Assays indicative of constitutive activity encompassed the canonical second messenger cAMP, activation of PKA and PKA-enhanced noradrenaline release; particularly the latter two provided for a highly sensitive measure of receptor activity, which we could record with no PDE inhibition. In contrast, inhibition of PDE was mandatory for the measurement of cAMP. In the absence of Ro20-1724, [^{3}H]cAMP was 270 ± 30 cpm, but 6,358 ± 423 cpm in its presence (three paired determinations), when formation (in cells pre-labelled with [^{3}H]adenine) was stimulated by CGS21680. Thus, PKA had a high sensitivity in registering receptor activity.

By contrast, constitutive receptor activity did not feed into alternative pathways that were independent of PKA. In SH cells stimulated by CGS21680, the PKA inhibitor reduced phosphorylation of CREB and of protein tyrosine residues only to moderate extent but did not inhibit phosphorylation of Rabphilin3A. In the presence of adenosine deaminase, the respective basal levels were unaffected by a receptor antagonist (not shown). When overexpressed in a surrogate cell line, the constitutive A_{2A}-receptor activity was similarly biased towards cAMP formation [30].

One less appreciated condition of A_{2A}-receptor signalling explored in our present study is signal partitioning. Our initial observation was that 8-Br-cAMP—as opposed to receptor-dependent cAMP—exhibited a dual effect. Similar to the receptor, 8-Br-cAMP caused release facilitation in a manner sensitive to the inhibition of PKA. By a second effect, 8-Br-cAMP elicited a significant reduction in noradrenaline release, refractory to the PKA inhibitor. Suppression of release occurred in the presence of TTX, hence independent of action potentials. These findings therefore suggest that cyclic AMP-mediated inhibition occurred at the active (presynaptic) zone. We attribute this inhibition to the restricted calcium current [42], which followed depolarisation in the presence of 8-Br-cAMP, but not of the A_{2A}-receptor agonist.

Presynaptic inhibition has recently been proposed to result from cAMP-enhanced gating of HCN channels and an ensuing inhibition of associated calcium channels [56]. Our data, however, point to a role of Src-family kinases. Previous reports have demonstrated Src-dependent release inhibition in neuronal cells [44–46]. A consequence of Src-kinase activity may be the restriction of VDCC with calcium channels and/or HCN representing potential phosphorylation substrates [57, 58]. In SH cells, there is ongoing Src activity, which is

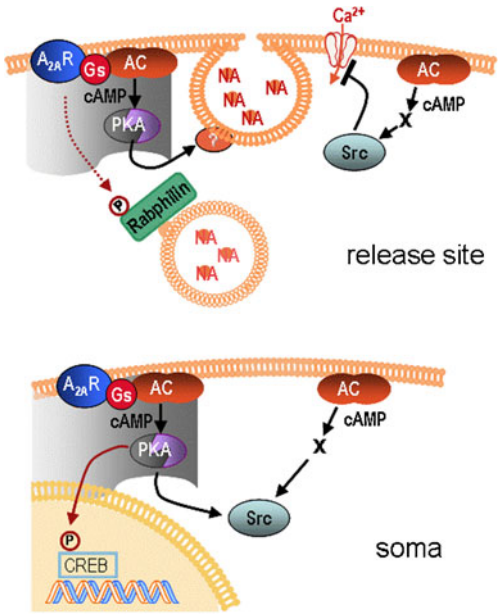

Fig. 8 Schematic representation of A_{2A}-receptor actions in SH-SY5Y cells. *Top*—at cellular release sites, cAMP formed within receptor-aligned signalling compartments (*grey area*) facilitated noradrenaline release by activating PKA (which primes vesicles for exocytosis, ref. [16]). Cyclic AMP produced outside receptor-signalling compartments enhanced Src-family kinase activity, restricted calcium influx and led to the inhibition of noradrenaline release. Phosphorylation of Rabphilin3A following receptor activation (*dotted arrow*) was independent of cAMP/PKA. *Bottom*—at regions beyond release sites (*soma*), A_{2A}-receptor activation caused phosphorylation of CREB and Src activation. Both effects were mediated in part by cAMP/PKA. Activation of Src by receptor-independent cAMP was via an unidentified pathway (*X*) bypassing PKA

instrumental during differentiation [59]. The Src inhibitor PP1 relieved release inhibition due to cAMP, but did not affect basal or cAMP-facilitated release; similarly, it suppressed CREB (serine 133) phosphorylation evoked by 8-Br-cAMP, but not by the receptor. Thus, the Src inhibitor discriminated between signalling of receptor-dependent and receptor-independent cAMP. At release sites, 8-Br-cAMP activated PKA to enhance noradrenaline release and in addition enhanced Src activity mediating inhibition.

Our data can be interpreted such that there are two signalling pathways relaying opposite effects; partitioning of these two signals may be due to the presence of subcellular compartments (illustrated in Fig. 8). We presume that in differentiated SH cells, compartments align to the A_{2A}-receptor and direct PKA to its cognate substrates (in the active zone, e.g. Rim1α, Snap 25, cf. [16]) and that, conversely, the inhibitory effect produced by 8-Br-cAMP or forskolin takes place outside compartment boundaries. Although the microscopic resolution of PKA–FRET was too low to outline compartment contours, the confinement of receptor-dependent cAMP transpired from PKA–FRET changes induced by 8-Br-cAMP. These changes also occurred in regions where there was no response to the receptor (cf. Fig. 3c).

Compartments are thought to form around an organising structure consisting of protein complexes that hold in apposition adenylyl cyclase, phosphodiesterase, protein kinases, phosphatases and their respective substrates; the protein complexes are sequestered through interaction with membrane-bound or cytoskeletal elements [17, 60]. In our SH cells, repeated RNA analysis predicts gravin/AKAP12 to be expressed (data not shown). AKAP12 is anchored to actin neurofilament as is α-actinin; the latter has been shown to bind to the A_{2A}-receptor, and thus may be responsible for integrating the receptor with the complex [61]. If, however, compartment architecture in a given cell excluded the receptor, it would be conceivable that receptor activity resulted in release inhibition whereas receptor-independent cAMP produced facilitation. Indeed, in synaptosomes from rat striatum, the A_{2A}-receptor was reported to inhibit release in a PKA-independent manner whereas PKA activation by 8-Br-cAMP enhanced release of γ-aminobutyric acid [62]; hence, the roles of receptor activation and of receptor-independent cAMP are inversely distributed relative to the situation in SH cells.

Taken together, our data show that differentiated SH cells, an established nerve cell model with a high degree of cellular homogeneity, express functional A_{2A}-receptors. Effector coupling is sensitive enough to register both agonist-stimulated and constitutive activity of the receptor; the latter accounts for a significant fraction (~20 %) of basal noradrenaline release The total A_{2A}-receptor effect is in keeping with data from the literature [14]. Our findings demonstrate that the native human A_{2A} adenosine receptor acts from a presynaptic site to regulate neurotransmitter release.

Acknowledgements The authors wish to thank their colleague Dr Sonja Sucic for assistance in the preparation of the manuscript. Work was supported by funding from FWF, the Austrian Science Fund (P 18150).

References

1. Haas HL, Selbach O (2000) Functions of neuronal adenosine receptors. Naunyn Schmiedebergs Arch Pharmacol 362:375–381
2. Cunha RA (2001) Adenosine as a neuromodulator and as a homeostatic regulator in the nervous system: different roles, different sources and different receptors. Neurochem Int 38:107–125
3. Ferré S, Quiroz C, Woods AS, Cunha R, Popoli P, Ciruela F, Lluis C, Franco R, Azdad K, Schiffmann SN (2008) An update on adenosine A2A-dopamine D2 receptor interactions: implications for the function of G protein-coupled receptors. Curr Pharm Des 14:1468–1474
4. Azdad K, Gall D, Woods AS, Ledent C, Ferré S, Schiffmann SN (2009) Dopamine D2 and adenosine A2A receptors regulate NMDA-mediated excitation in accumbens neurons through A2A–D2 receptor heteromerization. Neuropsychopharmacol 34:972–986
5. Sebastião AM, Ribeiro JA (1996) Adenosine A2 receptor-mediated excitatory actions on the nervous system. Prog Neurobiol 48:167–189
6. Popoli P, Betto P, Reggio R, Ricciarello G (1995) Adenosine A2A receptor stimulation enhances striatal extracellular glutamate levels in rats. Eur J Pharmacol 287:215–217
7. Kurokawa M, Koga K, Kase H, Nakamura J, Kuwana Y (1996) Adenosine A_{2a}-receptor-mediated modulation of striatal acetylcholine release in vivo. J Neurochem 66:1882–1888
8. Wirkner K, Gerevich Z, Krause T, Günther A, Köles L, Schneider D, Nörenberg W, Illes P (2004) Adenosine A2A receptor-induced inhibition of NMDA and $GABA_A$ receptor-mediated synaptic currents in a subpopulation of rat striatal neurons. Neuropharmacol 46:994–1007
9. Gomes CA, Vaz SH, Ribeiro JA, Sebastião AM (2006) Glial cell line-derived neurotrophic factor (GDNF) enhances dopamine release from striatal nerve endings in an adenosine A2A receptor-dependent manner. Brain Res 1113:129–136
10. Mayfield RD, Suzuki F, Zahniser NR (1993) Adenosine A2a receptor modulation of electrically evoked endogenous GABA release from slices of rat globus pallidus. J Neurochem 60:2334–2337
11. Kirk IP, Richardson PJ (1994) Adenosine A2a receptor-mediated modulation of striatal [^{3}H]GABA and [^{3}H]acetylcholine release. J Neurochem 62:960–966
12. Mori A, Shindou T, Ichimura M, Nonaka H, Kase H (1996) The role of adenosine A2a receptors in regulating GABAergic synaptic transmission in striatal medium spiny neurons. J Neurosci 16:605–611
13. Chergui K, Bouron A, Normand E, Mulle C (2000) Functional GluR6 kainate receptors in the striatum: indirect downregulation of synaptic transmission. J Neurosci 20:2175–2182
14. Shindou T, Nonaka H, Richardson PJ, Mori A, Kase H, Ichimura M (2002) Presynaptic adenosine A2A receptors enhance GABAergic synaptic transmission via a cyclic AMP dependent mechanism in the rat globus pallidus. Br J Pharmacol 136:296–302
15. Shindou T, Richardson PJ, Mori A, Kase H, Ichimura M (2003) Adenosine modulates the striatal GABAergic inputs to the globus pallidus via adenosine A2A receptors in rats. Neurosci Lett 352:167–170
16. Seino S, Shibasaki T (2005) PKA-dependent and PKA-independent pathways for cAMP-regulated exocytosis. Physiol Rev 85:1303–1342
17. Szaszák M, Christian F, Rosenthal W, Klussmann E (2008) Compartmentalized cAMP signalling in regulated exocytic processes in non-neuronal cells. Cell Signal 20:590–601

18. Zhong N, Beaumont V, Zucker RS (2004) Calcium influx through HCN channels does not contribute to cAMP-enhanced transmission. J Neurophysiol 92:644–647
19. Neitz A, Mergia E, Eysel UT, Koesling D, Mittmann T (2011) Presynaptic nitric oxide/cGMP facilitates glutamate release via hyperpolarization-activated cyclic nucleotide-gated channels in the hippocampus. Eur J Neurosci 33:1611–1621
20. Klinger M, Freissmuth M, Nanoff C (2002) Adenosine receptors: G protein-mediated signalling and the role of accessory proteins. Cell Signal 14:99–108
21. Cunha RA, Ribeiro JA (2000) Adenosine A2A receptor facilitation of synaptic transmission in the CA1 area of the rat hippocampus requires protein kinase C but not protein kinase A activation. Neurosci Lett 289:127–130
22. Gardner AM, Olah ME (2003) Distinct protein kinase C isoforms mediate regulation of vascular endothelial growth factor expression by A2A adenosine receptor activation and phorbol esters in pheochromocytoma PC12 cells. J Biol Chem 278:15421–15428
23. Kubista H, Boehm S (2006) Molecular mechanisms underlying the modulation of exocytotic noradrenalinee release via presynaptic receptors. Pharmacol Ther 112:213–242
24. Sebastião AM, Ribeiro JA (2009) Tuning and fine-tuning of synapses with adenosine. Curr Neuropharmacol 7:180–194
25. Cristóvão-Ferreira S, Vaz SH, Ribeiro JA, Sebastião AM (2009) Adenosine A2A-receptors enhance GABA transport into nerve terminals by restraining PKC inhibition of GAT-1. J Neurochem 109:336–347
26. Smith FD, Langeberg LK, Scott JD (2006) The where's and when's of kinase anchoring. Trends Biochem Sci 31:316–323
27. Appert-Collin A, Baisamy L, Diviani D (2006) Regulation of g protein-coupled receptor signaling by a-kinase anchoring proteins. J Recept Signal Transduct Res 26:631–646
28. Johansson S (1994) Graded action potentials generated by differentiated human neuroblastoma cells. Acta Physiol Scand 151:331–341
29. Brown NA, Kemp JA, Seabrook GR (1994) Block of human voltage-sensitive Na+ currents in differentiated SH-SY5Y cells by lifarizine. Br J Pharmacol 113:600–606
30. Klinger M, Kuhn M, Just H, Stefan E, Palmer T, Freissmuth M, Nanoff C (2002) Removal of the carboxy terminus of the A2A-adenosine receptor blunts constitutive activity: differential effect on cAMP accumulation and MAP kinase stimulation. Naunyn Schmiedebergs Arch Pharmacol 366:287–298
31. Lissandron V, Terrin A, Collini M, D'Alfonso L, Chirico G, Pantano S, Zaccolo M (2005) Improvement of a FRET-based indicator for cAMP by linker design and stabilization of donor-acceptor interaction. J Mol Biol 354:546–555
32. Encinas M, Iglesias M, Liu Y, Wang H, Muhaisen A, Ceña V, Gallego C, Comella JX (2000) Sequential treatment of SH-SY5Y cells with retinoic acid and brain-derived neurotrophic factor gives rise to fully differentiated, neurotrophic factor-dependent, human neuron-like cells. J Neurochem 75:991–1003
33. Boehm S (1999) ATP stimulates sympathetic transmitter release via presynaptic P2X purinoceptors. J Neurosci 19:737–746
34. Charalambous C, Gsandtner I, Keuerleber S, Milan-Lobo L, Kudlacek O, Freissmuth M, Zezula J (2008) Restricted collision coupling of the A2A receptor revisited: evidence for physical separation of two signaling cascades. J Biol Chem 283:9276–9288
35. Feige JN, Sage D, Wahli W, Desvergne B, Gelman L (2005) PixFRET, an ImageJ plug-in for FRET calculation that can accommodate variations in spectral bleed-throughs. Microsc Res Tech 68:51–58
36. Lechner SG, Hussl S, Schicker KW, Drobny H, Boehm S (2005) Presynaptic inhibition via a phospholipase C- and phosphatidylinositol bisphosphate-dependent regulation of neuronal Ca^{2+} channels. Mol Pharmacol 68:1387–1396
37. Pankevych H, Korkhov V, Freissmuth M, Nanoff C (2003) Truncation of the A1 adenosine receptor reveals distinct roles of the membrane-proximal carboxyl terminus in receptor folding and G protein coupling. J Biol Chem 278:30283–30293
38. Vaughan PF, Peers C, Walker JH (1995) The use of the human neuroblastoma SH-SY5Y to study the effect of second messengers on noradrenaline release. Gen Pharmacol 26:1191–1201
39. Goodall AR, Danks K, Walker JH, Ball SG, Vaughan PF (1997) Occurrence of two types of secretory vesicles in the human neuroblastoma SH-SY5Y. J Neurochem 68:1542–1552
40. Sarkanen JR, Nykky J, Siikanen J, Selinummi J, Ylikomi T, Jalonen TO (2007) Cholesterol supports the retinoic acid-induced synaptic vesicle formation in differentiating human SH-SY5Y neuroblastoma cells. J Neurochem 102:1941–1952
41. Pousinha PA, Diogenes MJ, Ribeiro JA, Sebastião AM (2006) Triggering of BDNF facilitatory action on neuromuscular transmission by adenosine A2A receptors. Neurosci Lett 404:143–147
42. Boehm S, Huck S (1996) Inhibition of N-type calcium channels: the only mechanism by which presynaptic alpha 2-autoreceptors control sympathetic transmitter release. Eur J Neurosci 8:1924–1931
43. Fykse EM, Li C, Südhof TC (1995) Phosphorylation of rabphilin-3A by Ca2+/calmodulin- and cAMP-dependent protein kinases in vitro. J Neurosci 15:2385–2395
44. Ohnishi H, Yamamori S, Ono K, Aoyagi K, Kondo S, Takahashi M (2001) A src family tyrosine kinase inhibits neurotransmitter release from neuronal cells. Proc Natl Acad Sci U S A 98:10930–10935
45. Baldwin ML, Cammarota M, Sim ATR, Rostas JAP (2006) Src family tyrosine kinases differentially modulate exocytosis from rat brain nerve terminals. Neurochem Int 49:80–86
46. Vela J, Pérez-Millán MI, Becu-Villalobos D, Díaz-Torga G (2007) Different kinases regulate activation of voltage-dependent calcium channels by depolarization in GH3 cells. Am J Physiol Cell Physiol 293:C951–C959
47. Walker F, deBlaquiere J, Burgess AW (1993) Translocation of pp 60c-src from the plasma membrane to the cytosol after stimulation by platelet-derived growth factor. J Biol Chem 268:19552–19558
48. Murray D, Hermida-Matsumoto L, Buser CA, Tsang J, Sigal CT, Ben-Tal N, Honig B, Resh MD, McLaughlin S (1998) Electrostatics and the membrane association of Src: theory and experiment. Biochemistry 37:2145–2159
49. Yu VC, Hochhaus G, Chang FH, Richards ML, Bourne HR, Sadée W (1988) Differentiation of human neuroblastoma cells: marked potentiation of prostaglandin E-stimulated accumulation of cyclic AMP by retinoic acid. J Neurochem 51:1892–1899
50. Brooke RE, Deuchars J, Deuchars SA (2004) Input-specific modulation of neurotransmitter release in the lateral horn of the spinal cord via adenosine receptors. J Neurosci 24:127–137
51. Shindou T, Arbuthnott GW, Wickens JR (2008) Actions of adenosine A 2A receptors on synaptic connections of spiny projection neurons in the neostriatal inhibitory network. J Neurophysiol 99:1884–1889
52. Nanoff C, Jacobson KA, Stiles GL (1991) The A2 adenosine receptor: guanine nucleotide modulation of agonist binding is enhanced by proteolysis. Mol Pharmacol 39:130–135
53. Nanoff C, Stiles GL (1993) Solubilization and characterization of the A2-adenosine receptor. J Recept Res 13:961–973
54. Roka F, Brydon L, Waldhoer M, Strosberg AD, Freissmuth M, Jockers R, Nanoff C (1999) Tight association of the human Mel (1a)-melatonin receptor and G(i): precoupling and constitutive activity. Mol Pharmacol 56:1014–1024
55. Hervé D (2011) Identification of a specific assembly of the g protein golf as a critical and regulated module of dopamine and adenosine-activated cAMP pathways in the striatum. Front Neuroanat 5:1–9
56. Huang Z, Lujan R, Kadurin I, Uebele VN, Renger JJ, Dolphin AC, Shah MM (2011) Presynaptic HCN1 channels regulate Cav3.2 activity and neurotransmission at select cortical synapses. Nat Neurosci 14:478–486

57. Weiss JL, Burgoyne RD (2001) Voltage-independent inhibition of P/Q-type Ca2+ channels in adrenal chromaffin cells via a neuronal Ca2+ sensor-1-dependent pathway involves Src family tyrosine kinase. J Biol Chem 276:44804–44811
58. Zong X, Eckert C, Yuan H et al (2005) A novel mechanism of modulation of hyperpolarization-activated cyclic nucleotide-gated channels by Src kinase. J Biol Chem 280:34224–34232
59. Bjelfman C, Meyerson G, Cartwright CA, Mellström K, Hammerling U, Påhlman S (1990) Early activation of endogenous pp 60src kinase activity during neuronal differentiation of cultured human neuroblastoma cells. Mol Cell Biol 10:361–370
60. Beene DL, Scott JD (2007) A-kinase anchoring proteins take shape. Curr Opin Cell Biol 19:192–198
61. Burgueño J, Blake DJ, Benson MA et al (2003) The adenosine A2A receptor interacts with the actin-binding protein alpha-actinin. J Biol Chem 278:37545–37552
62. Kirk IP, Richardson PJ (1995) Inhibition of striatal GABA release by the adenosine A2a receptor is not mediated by increases in cyclic AMP. J Neurochem 64:2801–2809